Magnetic domain structures of focused ion beam-patterned cobalt films using scanning ion microscopy with polarization analysis

Jian Li and Carl Rau[a)]
Department of Physics and Astronomy, Rice Quantum Institute and Center for Nanoscience and Technology, Rice University, Houston, Texas 77251

(Presented on 6 January 2004)

Studies of magnetic domain distributions in patterned magnetic materials are of pivotal importance in the areas of ultrahigh density magnetic recording, MRAM design, and miniaturized magnetic sensor arrays. Scanning ion microscopy with polarization analysis (SIMPA) is used to perform *in situ* topographic and magnetic domain imaging and focused ion beam (FIB) patterning. For FIB-patterned 30 nm thick Co films, it is found that rectangular Co bars of sizes between 10–30 μm exhibit *S* type, whereas circular shaped magnetic elements show *C* type micromagnetic magnetization patterns. It is shown that SIMPA provides a simple way to directly identify different micromagnetic domain patterns. © *2004 American Institute of Physics.*
[DOI: 10.1063/1.1689433]

Quite recently, studies of magnetic domains and magnetic domain walls have received great attention, not only because of their theoretical and experimental interest in studying a wealth of fundamental magnetization structures that emerge when one dimension of the sample is of the order of the bulk Bloch wall thickness, but also because of their pivotal importance for the development of highly sophisticated magnetic devices. Presently, nano- and micron-sized magnetic elements are being explored for their practical use for ultrahigh density magnetic storage, for magnetic reading and writing heads and for magnetic sensor arrays. Central to the exploration of these magnetic elements is the study of the mechanism of magnetization reversal via the formation of distinct magnetic domain and domain wall structures. Strong theoretical and experimental efforts are being made to explore these structures, which are often based on soft magnetic materials, such as polycrystalline Co and NiFe.[1–7]

In their study to explain switching field fluctuations of patterned magnetic elements, Zheng and Zhu[7] reported on two remanent magnetization patterns of a Co element, so-called *C* and *S* states, which possess different switching fields and switching behavior. Shi and Tehrani[8] found that during the magnetization reversal of patterned NiFeCo structures, edge-pinned states are formed which possess an increased switching field. Schabes and Bertram[9] reported on curling states, such as flower states and vortex states. For a recent review on magnetization patterns of thin-film elements, we refer to an article by Rave and Hubert.[4]

At present, there are no direct measurements of the magnetization distribution of *C* and *S* states, where the direction of the magnetization changes continuously. They were either predicted from micromagnetic computer simulations or indirectly deduced from magnetic measurements.[3,4]

We note that these different magnetic structures depend strongly on the material and shape, size, thickness and crystallographic microstructure of the magnetic elements. Therefore, it is advantageous not only to employ experimental methods that are able to detect changes of the vectorial orientation and magnitude of the magnetization at the surface of the elements, but also their surface topographic structure. Using scanning ion microscopy with polarization analysis (SIMPA), we have already reported on the pinning of magnetic domains at surface defects that are directly visible in the topographical images obtained from the ion microscope.[10] In SIMPA, a focused ion beam is scanned across a magnetic or nonmagnetic surface of a sample causing the ion-induced emission of spinpolarized or non-spinpolarized electrons. The magnitude and orientation of the spin polarization *P* of the ion-induced, emitted electrons is directly proportional to the magnitude and orientation of the magnetization of the local surface area probed by the focused ion beam. A magnetic image of the surface is then obtained by rastering the ion beam across the magnetic surface.

Here, we report on the investigation of the magnetic structure of *C* and *S* states obtained at surfaces of 30 nm thin, patterned, polycrystalline Co elements.

30 nm thick Co films are evaporated by using electron beam evaporation at a rate of 0.03 nm/s on Si(100) substrates as described elsewhere.[11] The Co/Si(100) samples are then inserted in a ultrahigh vacuum (UHV) chamber, where the longitudinal magneto-optical Kerr (MOKE) effect is studied. From all samples studied so far, we find perfectly square magnetic hysteresis loops with a coercivity field of 14.8 Oe. No change of size and shape of the square loops is observed upon rotation of the sample around the surface normal, which indicates the presence of zero or randomly oriented magnetocrystalline anisotropy due to the very good polycrystalline nature of the Co films.

Subsequently, the samples are transferred *in situ* from the MOKE chamber to the SIMPA microscope,[10] which is located in an UHV chamber operating in the low 10^{-10} mbar

a)Author to whom correspondence should be addressed; electronic mail: rau@rice.edu

FIG. 1. Magnetic domain image (size: 200 μm×140 μm) of the surface of a 30 nm thick Co/Si(100) film with a magnetic element of size 30 μm×21 μm created by ion beam milling and color wheel in the lower left part of the figure.

FIG. 2. Enlarged magnetic image of the ion beam created magnetic element of size 30 μm×21 μm.

region. This chamber houses a scanning, microfocused (minimum spot size: 35 nm) 6–30 keV Ga^+ ion beam facility, which is used to scan magnetic and nonmagnetic surfaces to induce the emission of secondary electrons from the sample surface. By using an extraction lens system and a Mott detector, the orientation and magnitude of the spin polarization P of the emitted electrons is analyzed in order to obtain images of magnetic domains and domain walls. The SIMPA technique offers some unique advantages compared to many other magnetic imaging techniques, because of its capability to produce vectorial maps of the surface magnetization by directly measuring the spatially resolved vector orientation and magnitude of P, which is a characteristic of the surface magnetization.[10] For fast adjustment of imaging parameters and precise location of surface areas to be imaged, a conventional electron detector is used to display topographic images on a TV monitor at TV rates. For further details, we refer to Refs. 10 and 12.

Rectangular, square and disk shaped magnetic elements of sizes between 10 and 30 μm are fabricated by ion beam milling. The magnetic structure can then immediately be studied *in situ* by using SIMPA.[10] For SIMPA imaging, typical ion currents are in the range of 0.1 nA or less, whereas for ion beam milling typical currents are in the nA range.

Figure 1 shows a magnetic domain image of the surface of a 30 nm thick Co/Si(100) film. Before magnetic imaging, the sample is demagnetized and a 30 μm×21 μm size magnetic element with rounded edges is created by ion beam etching. The white frame around the magnetic element represents an image of the zero polarization P of electrons emitted from the Si(100) substrate. The colors in the image represent different orientations of the in-plane polarization P as given by the color wheel (see inset in Fig. 1). The local distribution of P vectors is shown by white arrows. In order to obtain a clear plot of the P vectors and to account for statistical fluctuations in the electron count rates, P is first averaged over four nearest neighbors and then only every sixteenth P vector is plotted, thereby reducing the density of P vectors by a factor of 64. Clearly visible in the image is an 180° domain wall dividing the red and green shaped areas. The continuous rotation of the P vectors by 180° can be easily seen.

Figure 2 shows an enlarged image of the magnetic element shown in the center of Fig. 1. Here, the density of the P vectors is reduced by a factor of 16 in order to give a clear plot. From this plot, the existence of a magnetic S state is clearly visible. We note that such S states are also found in many similar shaped magnetic elements of sizes between 10 and 30 μm and aspect ratios close to 0.707.

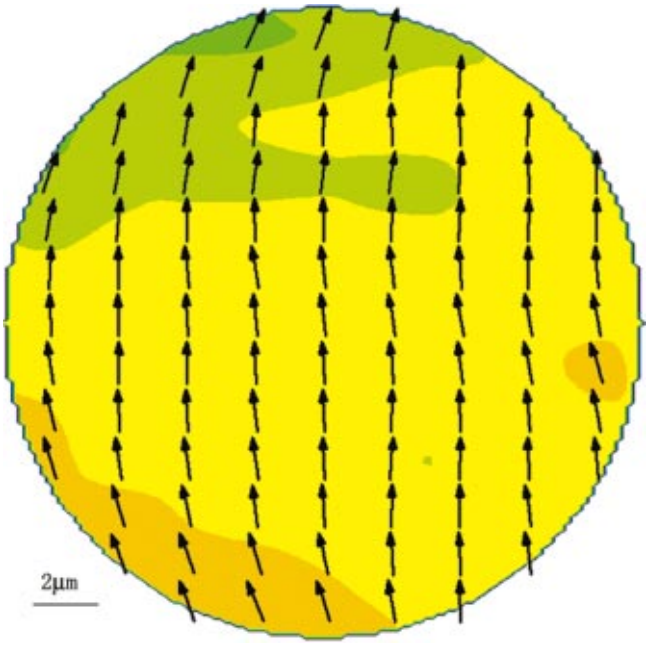

FIG. 3. Magnetic domain image of a circular (20 μm diameter) Co element, which was obtained after creating the element by ion beam milling and subsequently magnetizing the sample to saturation and then bringing it to the remanent state. For this image, the color wheel (see lower left part of Fig. 1) is slightly rotated to enable a simplified identification of the *C* state.

Figure 3 shows a magnetic image of a circular magnetic element (20 μm diameter) created by ion beam milling from a 30 nm thick Co/Si(100) film. Before imaging, the element is first created by ion beam etching and then magnetized to saturation and then brought to the remanent state. The *C* shaped magnetization configuration can be easily seen from the green shaped (upper left part of Fig. 3) and brown shaped (lower left part of Fig. 3) part of the image. In order to obtain a clear plot, the density of the blue *P* vectors is reduced by a factor of 16, thereby making the *C* state easily visible. Here, the color wheel (see lower left part of Fig. 1) is slightly rotated to allow for simplified identification of the *C* state.

We note that, from our SIMPA experiments, vortex and antivortex states are also found, which will be reported elsewhere.[12]

We have performed zero-temperature, micromagnetic simulations by using the OOMMF code.[13] As parameters for the various, 10–30 μm-sized magnetic elements of Co we used for the exchange constant $A = 1.55\ \mu$erg/cm, and for the saturation magnetization $M_s = 1414$ emu/cm^3.[14] As clearly indicated from the results of our MOKE data, the magnetocrystalline anisotropy constant K can be set to zero. From these simulations, only multi-domain and no quasistable *S* or *C* states could be generated.

In conclusion, we have shown that micromagnetic configurations such as *S* and *C* states exist in focused ion beam patterned, high quality, polycrystalline, 30 nm thick Co/Si(100) films. The experiments give clear evidence that SIMPA provides an excellent means to study micromagnetic configurations. The measured vectorial maps of the surface magnetization of the Co samples allow a detailed observation of magnetic domains and domain walls. The disagreement between the experimental findings and the numerical computations points to the fact that surface irregularities and crystal defects should be included in micromagnetic calculations in order to predict realistic magnetization patterns occurring during various stages of the magnetic treatment (saturation, demagnetization, reversal of magnetization) of magnetic samples. This is in agreement with Aharoni,[15] who proposed that crystal imperfections should be included in realistic micromagnetic calculations. We note that, at present, there is no experimental information available on the influence of a possible damage at the edges of the elements, caused by ion beam milling, which could affect the domain structure.

The authors are very grateful to J. Shi and D. Wu of the University of Utah for providing Co samples.

[1] J. Miltat, in *Applied Magnetism*, edited by R. Gerber, C. D. Wright, and G. Asti, Nato ASI Series E: Applied Sciences, Vol. 253 (Kluwer, Dordrecht, Netherlands, 1994).
[2] A. Hubert and R. Schäfer, *Magnetic Domains: The Analysis of Magnetic Microstructures* (Springer, Berlin, 1998).
[3] B. Heinrich, Can. J. Phys. **78**, 161 (2000).
[4] W. Rave and A. Hubert, IEEE Trans. Magn. **36**, 3886 (2000).
[5] G. Yi, P. R. Aitchison, W. D. Doyle, J. N. Chapman, and C. D. W. Wilkinson, J. Appl. Phys. **92**, 6087 (2002).
[6] B. Warot and A. K. Petford-Long, J. Appl. Phys. **93**, 7287 (2003).
[7] Y. Zheng and J.-G. Zhu, J. Appl. Phys. **81**, 5471 (1997).
[8] J. Shi and S. Tehrani, Appl. Phys. Lett. **77**, 1692 (2000).
[9] M. E. Schabes and H. N. Bertram, J. Appl. Phys. **64**, 1347 (1988).
[10] N. J. Zheng and C. Rau, Mater. Res. Soc. Symp. Proc. **313**, 723 (1993).
[11] W. C. Uhlig *et al.*, J. Appl. Phys. **91**, 6943 (2002).
[12] J. Li and C. Rau (unpublished).
[13] The OOMMF code is available for public use at ⟨http://math.nist.gov/oommf⟩.
[14] R. E. Dunin-Borkowski *et al.*, Appl. Phys. Lett. **75**, 2641 (1999).
[15] A. Aharoni, J. Magn. Magn. Mater. **203**, 33 (1999).